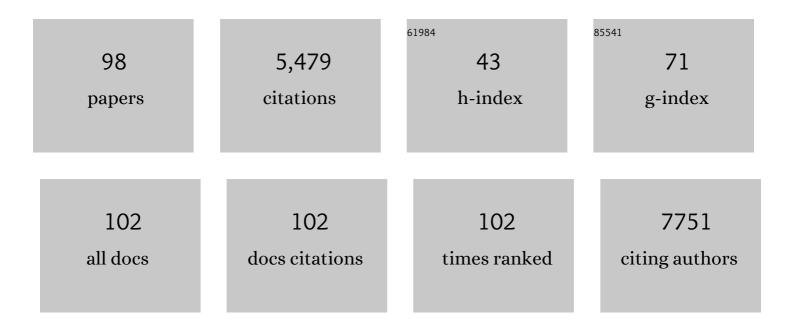
Xiaobing Zuo

List of Publications by Year in descending order

Source: https://exaly.com/author-pdf/2458897/publications.pdf Version: 2024-02-01



#	Article	IF	CITATIONS
1	Efficient blue light-emitting diodes based on quantum-confined bromide perovskite nanostructures. Nature Photonics, 2019, 13, 760-764.	31.4	483
2	A high-energy and long-cycling lithium–sulfur pouch cell via a macroporous catalytic cathode with double-end binding sites. Nature Nanotechnology, 2021, 16, 166-173.	31.5	392
3	Au ₁₃₃ (SPh- <i>t</i> Bu) ₅₂ Nanomolecules: X-ray Crystallography, Optical, Electrochemical, and Theoretical Analysis. Journal of the American Chemical Society, 2015, 137, 4610-4613.	13.7	265
4	Nanostructured Layered Cathode for Rechargeable Mg-Ion Batteries. ACS Nano, 2015, 9, 8194-8205.	14.6	181
5	Recognition of Multivalent Histone States Associated with Heterochromatin by UHRF1 Protein. Journal of Biological Chemistry, 2011, 286, 24300-24311.	3.4	177
6	Structurally Defined Nanoscale Sheets from Self-Assembly of Collagen-Mimetic Peptides. Journal of the American Chemical Society, 2014, 136, 4300-4308.	13.7	126
7	Quantitative 3D evolution of colloidal nanoparticle oxidation in solution. Science, 2017, 356, 303-307.	12.6	125
8	Parasitic Reactions in Nanosized Silicon Anodes for Lithium-Ion Batteries. Nano Letters, 2017, 17, 1512-1519.	9.1	122
9	Dynamics and Energetics of Single-Step Hole Transport in DNA Hairpins. Journal of the American Chemical Society, 2003, 125, 4850-4861.	13.7	120
10	DNA as Helical Ruler:Â Exciton-Coupled Circular Dichroism in DNA Conjugates. Journal of the American Chemical Society, 2005, 127, 14445-14453.	13.7	115
11	Optically Active BINOL Core-Based Phenyleneethynylene Dendrimers for the Enantioselective Fluorescent Recognition of Amino Alcohols. Journal of Organic Chemistry, 2001, 66, 6136-6140.	3.2	112
12	Rational Design of Helical Nanotubes from Self-Assembly of Coiled-Coil Lock Washers. Journal of the American Chemical Society, 2013, 135, 15565-15578.	13.7	112
13	An Unusual Topological Structure of the HIV-1 Rev Response Element. Cell, 2013, 155, 594-605.	28.9	109
14	X-ray diffraction "fingerprinting" of DNA structure in solution for quantitative evaluation of molecular dynamics simulation. Proceedings of the National Academy of Sciences of the United States of America, 2006, 103, 3534-3539.	7.1	100
15	Solution structure of the cap-independent translational enhancer and ribosome-binding element in the 3 [′] UTR of turnip crinkle virus. Proceedings of the National Academy of Sciences of the United States of America, 2010, 107, 1385-1390.	7.1	89
16	Relationship between Interchain Interaction, Exciton Delocalization, and Charge Separation in Low-Bandgap Copolymer Blends. Journal of the American Chemical Society, 2014, 136, 10024-10032.	13.7	88
17	Supramolecular Polymers in Aqueous Medium: Rational Design Based on Directional Hydrophobic Interactions. Journal of the American Chemical Society, 2011, 133, 16201-16211.	13.7	84
18	Orientation Control of Fluorescence Resonance Energy Transfer Using DNA as a Helical Scaffold. Journal of the American Chemical Society, 2005, 127, 10002-10003.	13.7	83

#	Article	IF	CITATIONS
19	Structure of the yeast U2/U6 snRNA complex. Rna, 2012, 18, 673-683.	3.5	78
20	Exploring the Programmable Assembly of a Polyoxometalate–Organic Hybrid via Metal Ion Coordination. Journal of the American Chemical Society, 2013, 135, 13425-13432.	13.7	78
21	Coordinative Self-Assembly and Solution-Phase X-ray Structural Characterization of Cavity-Tailored Porphyrin Boxes. Journal of the American Chemical Society, 2008, 130, 836-838.	13.7	75
22	Hydrophobic Dimerization and Thermal Dissociation of Perylenediimide-Linked DNA Hairpins. Journal of the American Chemical Society, 2009, 131, 5920-5929.	13.7	69
23	Structurally Homogeneous Nanosheets from Selfâ€Assembly of a Collagenâ€Mimetic Peptide. Angewandte Chemie - International Edition, 2014, 53, 8367-8371.	13.8	68
24	Efficient light-emitting diodes based on oriented perovskite nanoplatelets. Science Advances, 2021, 7, eabg8458.	10.3	68
25	Multiple conformations of SAM-II riboswitch detected with SAXS and NMR spectroscopy. Nucleic Acids Research, 2012, 40, 3117-3130.	14.5	67
26	Super-Stable, Highly Monodisperse Plasmonic Faradaurate-500 Nanocrystals with 500 Gold Atoms: Au _{â^1⁄4500} (SR) _{â^1⁄4120} . Journal of the American Chemical Society, 2014, 136, 7410-742	$1^{\frac{13.7}{17.7}}$	67
27	Faradaurate-940: Synthesis, Mass Spectrometry, Electron Microscopy, High-Energy X-ray Diffraction, and X-ray Scattering Study of Au _{â^¼940A±20} (SR) _{â^¼160A±4} Nanocrystals. ACS Nano 2014, 8, 6431-6439.	, 14.6	66
28	A Method for Helical RNA Global Structure Determination in Solution Using Small-Angle X-Ray Scattering and NMR Measurements. Journal of Molecular Biology, 2009, 393, 717-734.	4.2	65
29	Regulating the Hidden Solvationâ€lonâ€Exchange in Concentrated Electrolytes for Stable and Safe Lithium Metal Batteries. Advanced Energy Materials, 2020, 10, 2000901.	19.5	65
30	DNA-Mediated Exciton Coupling and Electron Transfer between Donor and Acceptor Stilbenes Separated by a Variable Number of Base Pairs. Journal of the American Chemical Society, 2004, 126, 8206-8215.	13.7	64
31	Helical Antimicrobial Sulfono-Î ³ -AApeptides. Journal of Medicinal Chemistry, 2015, 58, 4802-4811.	6.4	63
32	Structurally Ordered Nanowire Formation from Co-Assembly of DNA Origami and Collagen-Mimetic Peptides. Journal of the American Chemical Society, 2017, 139, 14025-14028.	13.7	59
33	Global Molecular Structure and Interfaces:  Refining an RNA:RNA Complex Structure Using Solution X-ray Scattering Data. Journal of the American Chemical Society, 2008, 130, 3292-3293.	13.7	54
34	Self-Recognition of Structurally Identical, Rod-Shaped Macroions with Different Central Metal Atoms during Their Assembly Process. Journal of the American Chemical Society, 2013, 135, 4529-4536.	13.7	54
35	Structured m <scp>RNA</scp> induces the ribosome into a hyperâ€rotated state. EMBO Reports, 2014, 15, 185-190.	4.5	53
36	Self-Assembly of an α-Helical Peptide into a Crystalline Two-Dimensional Nanoporous Framework. Journal of the American Chemical Society, 2016, 138, 16274-16282.	13.7	53

#	Article	IF	CITATIONS
37	Resolving Conflicting Crystallographic and NMR Models for Solution-State DNA with Solution X-ray Diffraction. Journal of the American Chemical Society, 2005, 127, 16-17.	13.7	51
38	Dynamics of Inter- and Intrastrand Hole Transport in DNA Hairpins. Journal of the American Chemical Society, 2002, 124, 4568-4569.	13.7	50
39	Stepwise Evolution of the Structure and Electronic Properties of DNA. Journal of the American Chemical Society, 2003, 125, 12729-12731.	13.7	50
40	Determination of Multicomponent Protein Structures in Solution Using Global Orientation and Shape Restraints. Journal of the American Chemical Society, 2009, 131, 10507-10515.	13.7	50
41	Two ZnF-UBP Domains in Isopeptidase T (USP5). Biochemistry, 2012, 51, 1188-1198.	2.5	49
42	Self-assembly of aramid amphiphiles into ultra-stable nanoribbons and aligned nanoribbon threads. Nature Nanotechnology, 2021, 16, 447-454.	31.5	49
43	Solution-Phase Structural Characterization of Supramolecular Assemblies by Molecular Diffraction. Journal of the American Chemical Society, 2007, 129, 1578-1585.	13.7	47
44	Photocatalytic probing of DNA sequence by using TiO2/dopamine-DNA triads. Chemical Physics, 2007, 339, 154-163.	1.9	45
45	Rapid global structure determination of large RNA and RNA complexes using NMR and small-angle X-ray scattering. Methods, 2010, 52, 180-191.	3.8	44
46	Seeded Heteroepitaxial Growth of Crystallizable Collagen Triple Helices: Engineering Multifunctional Two-Dimensional Core–Shell Nanostructures. Journal of the American Chemical Society, 2019, 141, 20107-20117.	13.7	42
47	Supramolecular porphyrinic prisms: coordinative assembly and solution phase X-ray structural characterization. Chemical Communications, 2006, , 4581.	4.1	40
48	Small-angle X-ray scattering: a bridge between RNA secondary structures and three-dimensional topological structures. Current Opinion in Structural Biology, 2015, 30, 147-160.	5.7	40
49	Rational Design of Multilayer Collagen Nanosheets with Compositional and Structural Control. Journal of the American Chemical Society, 2015, 137, 7793-7802.	13.7	40
50	2D Crystal Engineering of Nanosheets Assembled from Helical Peptide Building Blocks. Angewandte Chemie - International Edition, 2019, 58, 13507-13512.	13.8	39
51	Activated Decay Pathways for Planar vs Twisted Singlet Phenylalkenes. Journal of the American Chemical Society, 2003, 125, 8806-8813.	13.7	35
52	Native State Volume Fluctuations in Proteins as a Mechanism for Dynamic Allostery. Journal of the American Chemical Society, 2017, 139, 3599-3602.	13.7	33
53	Symmetry-Enforced Conformational Control of Photochemical Reactivity in 2-Vinyl-1,3-terphenyl. Journal of the American Chemical Society, 2002, 124, 13664-13665.	13.7	32
54	Structural Basis of Focal Adhesion Localization of LIM-only Adaptor PINCH by Integrin-linked Kinase. Journal of Biological Chemistry, 2009, 284, 5836-5844.	3.4	32

#	Article	IF	CITATIONS
55	Ambidextrous helical nanotubes from self-assembly of designed helical hairpin motifs. Proceedings of the United States of America, 2019, 116, 14456-14464.	7.1	32
56	Sulfonoâ€Î³â€AApeptides as a New Class of Nonnatural Helical Foldamer. Chemistry - A European Journal, 2015, 21, 2501-2507.	3.3	30
57	Relaxation Pathways of Photoexcited Diaminostilbenes. Themeta-Amino Effect. Journal of Physical Chemistry A, 2001, 105, 4691-4696.	2.5	28
58	Helical 1:1 α/Sulfono-γ-AA Heterogeneous Peptides with Antibacterial Activity. Biomacromolecules, 2016, 17, 1854-1859.	5.4	28
59	Incorporation of isotopic, fluorescent, and heavy-atom-modified nucleotides into RNAs by position-selective labeling of RNA. Nature Protocols, 2018, 13, 987-1005.	12.0	27
60	Shape-Shifting Peptide Nanomaterials: Surface Asymmetry Enables pH-Dependent Formation and Interconversion of Collagen Tubes and Sheets. Journal of the American Chemical Society, 2020, 142, 19956-19968.	13.7	27
61	Simulation of voltammogram on rough electrode. Electrochimica Acta, 1997, 42, 2555-2558.	5.2	26
62	New Class of Heterogeneous Helical Peptidomimetics. Organic Letters, 2015, 17, 3524-3527.	4.6	26
63	Structural Architecture of Prothrombin in Solution Revealed by Single Molecule Spectroscopy. Journal of Biological Chemistry, 2016, 291, 18107-18116.	3.4	26
64	Torsional Barriers for Planar versus Twisted Singlet Styrenes. Journal of the American Chemical Society, 2003, 125, 2046-2047.	13.7	23
65	Conformer-specific photoisomerizaton of some 2-vinylbiphenyls. Photochemical and Photobiological Sciences, 2003, 2, 1059-1066.	2.9	23
66	X-ray scattering combined with coordinate-based analyses for applications in natural and artificial photosynthesis. Photosynthesis Research, 2009, 102, 267-279.	2.9	23
67	Crystal structure of tripleâ€BRCTâ€domain of ECT2 and insights into the binding characteristics to CYKâ€4. FEBS Letters, 2014, 588, 2911-2920.	2.8	22
68	Huntingtin structure is orchestrated by HAP40 and shows a polyglutamine expansion-specific interaction with exon 1. Communications Biology, 2021, 4, 1374.	4.4	22
69	Competitive 1,2- and 1,5-Hydrogen Shifts Following 2-Vinylbiphenyl Photocyclization. Journal of Organic Chemistry, 2005, 70, 10447-10452.	3.2	20
70	Characterization of Protein Flexibility Using Small-Angle X-Ray Scattering and Amplified Collective Motion Simulations. Biophysical Journal, 2014, 107, 956-964.	0.5	20
71	The J-elongated conformation of β2-glycoprotein I predominates in solution: implications for our understanding of antiphospholipid syndrome. Journal of Biological Chemistry, 2020, 295, 10794-10806.	3.4	20
72	Isolation of a 300 kDa, Au _{â^¼1400} Gold Compound, the Standard 3.6 nm Capstone to a Series of Plasmonic Nanocrystals Protected by Aliphatic-like Thiolates. Journal of Physical Chemistry Letters, 2018, 9, 6825-6832.	4.6	18

#	Article	IF	CITATIONS
73	Dynamics and Energetics of Hole Trapping in DNA by 7-Deazaguanine. Angewandte Chemie - International Edition, 2002, 41, 1026-1028.	13.8	17
74	Synchronous RNA conformational changes trigger ordered phase transitions in crystals. Nature Communications, 2021, 12, 1762.	12.8	17
75	Pseudoknot length modulates the folding, conformational dynamics, and robustness of Xrn1 resistance of flaviviral xrRNAs. Nature Communications, 2021, 12, 6417.	12.8	15
76	Au _{329–<i>x</i>} Ag _{<i>x</i>} (SR) ₈₄ Nanomolecules: Plasmonic Alloy Faradaurate-329. Journal of Physical Chemistry Letters, 2015, 6, 3320-3326.	4.6	13
77	Morphological Transitions of a Photoswitchable Aramid Amphiphile Nanostructure. Nano Letters, 2021, 21, 2912-2918.	9.1	13
78	Hydrothermal Conditioning of Physical Hydrogels Prepared from a Midblockâ€ S ulfonated Multiblock Copolymer. Macromolecular Rapid Communications, 2017, 38, 1600666.	3.9	12
79	Solvent dependent photocyclization and photophysics of some 2-ethynylbiphenyls. Photochemical and Photobiological Sciences, 2006, 5, 369.	2.9	11
80	2D Crystal Engineering of Nanosheets Assembled from Helical Peptide Building Blocks. Angewandte Chemie, 2019, 131, 13641-13646.	2.0	11
81	Enhancing the anticoagulant profile of meizothrombin. Biomolecular Concepts, 2018, 9, 169-175.	2.2	10
82	Determining structural ensembles of flexible multi-domain proteins using small-angle X-ray scattering and molecular dynamics simulations. Protein and Cell, 2015, 6, 619-623.	11.0	9
83	ssDNA-amphiphile architecture used to control dimensions of DNA nanotubes. Nanoscale, 2019, 11, 19850-19861.	5.6	8
84	Zymogen and activated protein C have similar structural architecture. Journal of Biological Chemistry, 2020, 295, 15236-15244.	3.4	8
85	Oblique angle deposition of boron carbide films by magnetron sputtering. Journal of Applied Physics, 2021, 130, .	2.5	8
86	Programmed Supramolecular Assemblies Using Orthogonal Pairs of Heterodimeric Coiled Coil Peptides. Angewandte Chemie - International Edition, 2022, 61, .	13.8	8
87	Stochastic resonance in liquid membrane oscillator. Journal of Chemical Physics, 1998, 109, 6063-6066.	3.0	7
88	Solution-State Conformational Ensemble of a Hexameric Porphyrin Array Characterized Using Molecular Dynamics and X-ray Scattering. Journal of Physical Chemistry A, 2009, 113, 2516-2523.	2.5	7
89	X-ray multi-probe data acquisition: A novel technique for laser pump x-ray transient absorption spectroscopy. Review of Scientific Instruments, 2021, 92, 085109.	1.3	7
90	Temperature-Dependent Photochemistry of 1,3-Diphenylpropenes. The Di-Ï€-Methane Reaction Revisited. Journal of the American Chemical Society, 2001, 123, 11883-11889.	13.7	6

#	Article	IF	CITATIONS
91	Self-assembly of chimeric peptides toward molecularly defined hexamers with controlled multivalent ligand presentation. Chemical Communications, 2020, 56, 7128-7131.	4.1	4
92	The Di-π-methane Reaction of 3,3-Dimethyl-1,3-Diphenylpropene Revisited:  Dynamics and Barriers for Competitive Singlet State Reactions. Journal of the American Chemical Society, 2000, 122, 8571-8572.	13.7	3
93	The mechanism driving a solid–solid phase transition in a biomacromolecular crystal. IUCrJ, 2021, 8, 655-664.	2.2	2
94	X-ray Scattering for Bio-Molecule Structure Characterization. Advances in Photosynthesis and Respiration, 2008, , 151-165.	1.0	2
95	Programmed Supramolecular Assemblies using Orthogonal Pairs of Heterodimeric Coiled Coil Peptides. Angewandte Chemie, 0, , .	2.0	1
96	Starting over with Styrene. ChemInform, 2004, 35, no.	0.0	0
97	Ligand Induced Conformational Changes of Riboswitches Probed by SAXS and NMR Spectroscopy. Biophysical Journal, 2011, 100, 237a.	O.5	0
98	A Top-Down Approach to Determining Global RNA Structures in Solution Using NMR and Small-Angle	0.2	0

X-ray Scattering Measurements. Nucleic Acids and Molecular Biology, 2012, , 335-359. 98